

The effect of electron–hole scattering on the transport properties of a 2D semimetal in a HgTe quantum well

M.V. Entin¹, L.I. Magarill^{1,2}, E.B. Olshanetsky¹, Z.D. Kvon^{1,2}, N.N. Mikhailov¹, S.A. Dvoretzky¹

¹*Institute of Semiconductor Physics, Siberian Branch of the Russian Academy of Sciences, Novosibirsk, 630090, Russia*

²*Novosibirsk State University, Novosibirsk, 630090, Russia*

The influence of e-h scattering on the conductivity and magnetotransport of 2D semimetallic HgTe is studied both theoretically and experimentally. The presence of e-h scattering leads to the friction between electron and holes resulting in a large temperature-dependent contribution to the transport coefficients. The coefficient of friction between electrons and holes is determined. The comparison of experimental data with the theory shows that the interaction between electrons and holes based on the long - range Coulomb potential strongly underestimates the e-h friction. The experimental results are in agreement with the model of strong short-range e-h interaction.

PACS numbers:

Keywords:

Introduction

Recently a 2D semimetal has been shown to be present in undoped 18-21 nm HgTe quantum wells with an inverted energy spectrum and various surface orientations (013), (112) and (100) [1–3]. It has been shown that this semimetallic state is due to the overlap by an order of several meVs of the conduction band minimum in the center of the Brillouin zone and the valence band several maxima (the exact number and configuration depending on the well surface orientation) situated at some distance away from the Brillouin zone center. The Fermi energy residing inside the energy interval corresponding to this overlap results in a simultaneous existence of 2D electrons and holes in the QW. The technology of low-temperature growth of a composite (SiO_2/Si_3N_4) dielectric layer on top of the QWs has allowed the fabrication of electrostatic top gate. Using this gate makes it possible to obtain and study 2D semimetal states with any desired ratio of electron and hole densities. The study conducted in (013)-oriented HgTe wells has revealed certain features which are peculiar to the transport in a 2D semimetal and may be attributed to the electron–hole scattering inside the QW [4]. The present work presents a detailed theoretical and experimental study of electron–hole scattering in a 2D semimetal.

It is well known that in monopolar systems the interelectron scattering does not affect the low-field conductivity. The scattering between particles of the same kind conserves the total momentum of the system. The momentum generated by an external electric field does not dissipate, unless the impurities or phonons are involved. As a result, in a system with a simple electronic spectrum the conductivity does not depend on the electron–electron scattering. This is not the case in a multi-component system [5], [6]. In the absence of mutual collisions, the components drift in an external electric field with different velocities. The scattering between particles of different sorts leads to the additional friction in the whole system. In semimetal, electrons and holes

are accelerated by the electric field in the opposite directions and the collision between particles slows the motion of both electrons and holes. At low temperature the e-h scattering is limited (both for electrons and holes) to the kT interval near the Fermi surface resulting in the temperature dependence of the probability of e-h scattering and of the corresponding corrections to conductivity $\propto T^2$ [4]. (However, in systems with degenerate spectrum, e.g., in a 2D system in quantizing magnetic fields the e-h scattering is not frozen out down to zero temperature, see [7]). The paper is organized as follows. Section I contains the theory of electron–hole scattering in a 2D semimetal. Section II deals with the experimental details. In Section III the comparison between the theory and experiment is discussed.

I. THE THEORY OF ELECTRON–HOLE SCATTERING

Kinetic equation solution

We consider a 2D semimetal with the g_e equivalent electron valleys and g_h equivalent hole valleys centered in points $\mathbf{p}_{e,i}$ and $\mathbf{p}_{h,i}$, correspondingly. In particular, as will be discussed in the next section, for the (013) HgTe QW studied in the experiment we have a single conductance band valley in the center of the Brillouin zone and two valence band valleys situated along the $[0\bar{3}1]$ direction, Fig.1. The conduction bands with energy spectra $\varepsilon_{\mathbf{p}}^e = (\mathbf{p} - \mathbf{p}_{e,i})^2/2m_e$ overlaps with valence bands $E_g - \varepsilon_{\mathbf{p} - \mathbf{p}_{h,i}}^h$, $\varepsilon_{\mathbf{p}}^h = p^2/2m_h$ ($E_g > 0$). Hole mass m_h is assumed to be much larger than the electron mass m_e . The distances between electron and hole extrema $|\mathbf{p}_{h,i} - \mathbf{p}_{e,j}|$ are supposed to be large to suppress the electron–hole recombination. At the same time, the scattering between electrons and holes changing momenta near the extrema is permitted. Without the loss of generality, further we will count the momenta from the band extrema and replace $\mathbf{p} - \mathbf{p}_{h,j} \rightarrow \mathbf{p}$, $\mathbf{p} - \mathbf{p}_{e,i} \rightarrow \mathbf{p}$.

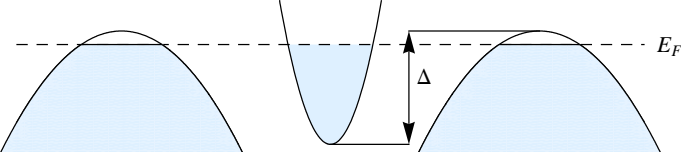


FIG. 1: The energy band structure in a 20 nm (013) HgTe quantum well.

The system of kinetic equations for the electron and hole distribution functions $f_{\mathbf{p}}^{e,h}$ reads

$$e_{\nu} \mathbf{E} \nabla_{\mathbf{p}} f_{\mathbf{p}}^{\nu} + [\mathbf{p}, \boldsymbol{\omega}_{\nu}] \nabla_{\mathbf{p}} f_{\mathbf{p}}^{\nu} = \sum_{\nu'} I_{\nu, \nu'} + J_{\nu}, \quad (1)$$

where index $\nu = (+, -)$ numerates holes (h) and electrons (e), respectively, $e_{\pm} = \pm e$, $-e$ is the electron charge, J_{ν} is the collision integral of holes (electrons) with impurities, $I_{\nu, \nu'}$ are the inter-particle collision integrals, $\boldsymbol{\omega}_{\nu} = e_{\nu} \mathbf{H} / m_{\nu} c$, ω_{ν} are cyclotron frequencies. In the linear conductivity problem the collision integrals for particles of the same sort ($I_{\nu, \nu}$) give no contribution to the conductivity. Hence, the summation over ν' can be omitted replacing ν' by $\bar{\nu} = -\nu$.

The hole-electron collision integral has the form

$$I_{he} = \frac{2\pi}{S^2} 2g_e \sum_{\mathbf{p}', \mathbf{q}, \mathbf{k}'} |u_{\mathbf{q}}|^2 \delta_{\mathbf{p}', \mathbf{p}+\mathbf{q}} \delta_{\mathbf{k}', \mathbf{k}+\mathbf{q}} \delta(\varepsilon_{\mathbf{p}}^h - \varepsilon_{\mathbf{p}'}^h + \varepsilon_{\mathbf{k}'}^e - \varepsilon_{\mathbf{k}}^e) \times \\ [f_{\mathbf{p}}^h (1 - f_{\mathbf{p}'}^h) f_{\mathbf{k}'}^e (1 - f_{\mathbf{k}}^e) - f_{\mathbf{p}'}^h (1 - f_{\mathbf{p}}^h) f_{\mathbf{k}}^e (1 - f_{\mathbf{k}'}^e)]. \quad (2)$$

Here $u_{\mathbf{q}}$ is the Fourier transform of the electron-hole interaction potential $u(\mathbf{r})$, S is the system area. Value I_{eh} can be obtained from Eq.(4) by exchange $e \rightleftharpoons h$.

We shall study linear (in \mathbf{E}) transport. Introducing linear corrections $\phi_{\mathbf{p}}^{\nu}$ to equilibrium distribution functions

$f_{\mathbf{p}}^{0, \nu}$ and linearizing the kinetic equations, we obtain

$$e_{\nu} (\mathbf{E} \nabla_{\mathbf{p}}) f_{\mathbf{p}}^{0\nu} + ([\mathbf{p}, \boldsymbol{\omega}_{\nu}] \nabla_{\mathbf{p}}) \phi_{\mathbf{p}}^{\nu} = \delta I_{\nu, \bar{\nu}} + \delta J_{\nu}, \quad (3)$$

where $\delta I_{\nu, \bar{\nu}}$ and δJ_{ν} are linearized collision integrals,

$$\delta I_{\nu, \bar{\nu}} = \frac{2\pi}{S^2} 2g_{\bar{\nu}} \sum_{\mathbf{p}', \mathbf{q}, \mathbf{k}'} |u_{\mathbf{q}}|^2 \delta_{\mathbf{p}', \mathbf{p}+\mathbf{q}} \delta_{\mathbf{k}', \mathbf{k}+\mathbf{q}} \delta(\varepsilon_{\mathbf{p}}^{\nu} - \varepsilon_{\mathbf{p}'}^{\nu} + \varepsilon_{\mathbf{k}'}^{\bar{\nu}} - \varepsilon_{\mathbf{k}}^{\bar{\nu}}) \times \\ \left\{ \phi_{\mathbf{p}}^{\nu} [(1 - f_{\mathbf{p}'}^{0\nu}) f_{\mathbf{k}'}^{0\bar{\nu}} (1 - f_{\mathbf{k}}^{0\bar{\nu}}) + f_{\mathbf{p}'}^{0\nu} f_{\mathbf{k}}^{0\bar{\nu}} (1 - f_{\mathbf{k}'}^{0\bar{\nu}})] - \phi_{\mathbf{p}'}^{\nu} [f_{\mathbf{p}}^{0\nu} f_{\mathbf{k}'}^{0\bar{\nu}} (1 - f_{\mathbf{k}}^{0\bar{\nu}}) + (1 - f_{\mathbf{p}}^{0\nu}) f_{\mathbf{k}}^{0\bar{\nu}} (1 - f_{\mathbf{k}'}^{0\bar{\nu}})] + \right. \\ \left. \phi_{\mathbf{k}'}^{\bar{\nu}} [f_{\mathbf{p}}^{0\nu} (1 - f_{\mathbf{p}'}^{0\nu}) (1 - f_{\mathbf{k}}^{0\bar{\nu}}) + f_{\mathbf{p}'}^{0\nu} (1 - f_{\mathbf{p}}^{0\nu}) f_{\mathbf{k}}^{0\bar{\nu}}] - \phi_{\mathbf{k}}^{\bar{\nu}} [(1 - f_{\mathbf{p}'}^{0\nu}) f_{\mathbf{k}'}^{0\bar{\nu}} f_{\mathbf{p}}^{0\nu} + f_{\mathbf{p}'}^{0\nu} (1 - f_{\mathbf{p}}^{0\nu}) (1 - f_{\mathbf{k}}^{0\bar{\nu}})] \right\}. \quad (4)$$

The solution of the system of kinetic equations can be searched in the form of $\phi_{\mathbf{p}}^{\nu} = \mathbf{A}^{\nu}(\varepsilon_{\mathbf{p}}) \mathbf{p}$, $\mathbf{A}^{\nu}(\varepsilon_{\mathbf{p}}) \propto \mathbf{E}$. This substitution results in the system of integral equations for $\mathbf{A}^{\nu}(\varepsilon_{\mathbf{p}})$. Instead of solving this system we use approximation

$$\phi_{\mathbf{p}}^{\nu} \approx -\mathbf{p} \mathbf{V}^{\nu} \partial_{\varepsilon_{\mathbf{p}}^{\nu}} f_{\mathbf{p}}^{(0\nu)}, \quad (5)$$

where \mathbf{V}^{ν} are the average velocities of particles. To find the values \mathbf{V}^{ν} one should integrate the kinetic equations with the momentum \mathbf{p} . The impurity collision term gives the rate of irretrievable momentum loss. The h-e collision term determines the rate of momentum transfer between holes and electrons (the force between subsystems

of holes and electrons)

$$\mathbf{f} = 2g_h \sum_{\mathbf{p}} \mathbf{p} I_{he}. \quad (6)$$

The considered procedure is equivalent to the algebraization of the collision terms

$$\delta J_{\nu} = -\frac{\phi^{\nu}}{\tau_{\nu}}, \quad \delta I_{\nu, \bar{\nu}} = \frac{\phi^{\bar{\nu}}}{\tau_{\bar{\nu}\nu}} - \frac{\phi^{\nu}}{\tau_{\nu\bar{\nu}}},$$

where τ_{ν} is the transport relaxation for elastic scattering on impurities. Relaxation times τ_{he} and τ_{eh} of interparticle scattering satisfy the relation

$$\frac{m_h}{N_s \tau_{he}} = \frac{m_e}{P_s \tau_{eh}} = \eta.$$

Quantity η can be considered as the coefficient of liquid friction between the subsystems of holes and electrons: the force between electrons and holes is $SN_sP_s\eta(\mathbf{V}^e - \mathbf{V}^h)$.

As a result we come to the system of hydrodynamic equations [5, 6] for \mathbf{V}^ν

$$\frac{e_\nu}{m_\nu}\mathbf{E} + [\mathbf{V}^\nu, \boldsymbol{\omega}_\nu] - \frac{\mathbf{V}^\nu}{\tau_\nu} - \eta \frac{n_{\bar{\nu}}}{m_\nu}(\mathbf{V}^\nu - \mathbf{V}^{\bar{\nu}}) = 0. \quad (7) \quad \text{where}$$

The system (7) can be written in the matrix form as

$$\Omega \cdot V = \mathcal{E}, \quad (8)$$

$$V = (V_x^e, V_y^e, V_x^h, V_y^h), \quad \mathcal{E} = e(E_x/m_e, E_y/m_e, -E_x/m_h, -E_y/m_h),$$

$$\Omega = \begin{pmatrix} -(\frac{1}{\tau_e} + \frac{1}{\tau_{eh}}) & \omega_e & \frac{1}{\tau_{eh}} & 0 \\ -\omega_e & -(\frac{1}{\tau_e} + \frac{1}{\tau_{eh}}) & 0 & \frac{1}{\tau_{eh}} \\ \frac{1}{\tau_{he}} & 0 & -(\frac{1}{\tau_h} + \frac{1}{\tau_{he}}) & \omega_h \\ 0 & \frac{1}{\tau_{he}} & -\omega_h & -(\frac{1}{\tau_h} + \frac{1}{\tau_{he}}) \end{pmatrix} \quad (9)$$

With the use of the solution of Eq.(9) $V = \Omega^{-1}\mathcal{E}$ we obtain $j_x = e(V_x^h P_s - V_x^e N_s)$, $j_y = e(V_y^h P_s - V_y^e N_s)$ and

$$\begin{aligned} \sigma_{xx} &= N_1/D, \quad \sigma_{yx} = N_2/D, \\ N_1 &= e^2 \left(m_e m_h (m_e P_s \tau_h (\tau_e^2 \omega_e^2 + 1) + m_h N_s \tau_e (\tau_h^2 \omega_h^2 + 1)) + \eta (2m_e m_h \tau_e \tau_h (N_s - P_s)^2 + \right. \\ &\quad \left. N_s P_s (\tau_e \tau_h \omega_e \omega_h + 1) + N_s P_s (m_h^2 \tau_e^2 (\tau_h^2 \omega_h^2 + 1) + m_e^2 \tau_h^2 (\tau_e^2 \omega_e^2 + 1)) \right) + \\ &\quad \eta^2 (N_s - P_s)^2 \tau_e \tau_h (m_h P_s \tau_e + m_e N_s \tau_h) \Big), \\ N_2 &= -e^2 \left(m_e m_h (m_h N_s \omega_e (\tau_h^2 \omega_h^2 + 1) \tau_e^2 + m_e P_s \tau_h^2 (\tau_e^2 \omega_e^2 + 1) \omega_h) + 2\eta m_e m_h \tau_e \tau_h \times \right. \\ &\quad \left. (N_s - P_s) (N_s \tau_e \omega_e - P_s \tau_h \omega_h) + \eta^2 \tau_e^2 \tau_h^2 (N_s - P_s)^2 (m_e N_s \omega_e + m_h P_s \omega_h) \right), \\ D &= m_e^2 m_h^2 (1 + \omega_e^2 \tau_e^2) (1 + \omega_h^2 \tau_h^2) + 2\eta m_e m_h (m_e N_s \tau_h (1 + \omega_e^2 \tau_e^2) + m_h P_s \tau_e (1 + \omega_h^2 \tau_h^2)) + \\ &\quad \eta^2 ((m_h P_s \tau_e + m_e N_s \tau_h)^2 + \tau_e^2 \tau_h^2 (m_e N_s \omega_e + m_h P_s \omega_e)^2). \end{aligned} \quad (10)$$

For components of resistivity tensor one can write

$$\rho_{xx} = \frac{N_1 D}{N_1^2 + N_2^2}, \quad \rho_{xy} = \frac{N_2 D}{N_1^2 + N_2^2}. \quad (11)$$

At zero magnetic field $\rho_{xy} = 0$, and the temperature-dependent correction to the resistivity are simplified

$$\delta\rho(T)/\rho(T=0) = \frac{m_h N_s \tau_e + m_e P_s \tau_h}{m_e m_h} \frac{m_e m_h + \eta (m_h P_s \tau_e + m_e N_s \tau_h)}{m_h N_s \tau_e + m_e P_s \tau_h + \eta \tau_e \tau_h (P_s - N_s)^2} - 1 \quad (12)$$

Electron-hole relaxation time

The mean force acting between electron and hole subsystems \mathbf{f} , Eq.(6), in the Born approximation is deter-

mined by substitution of the distribution functions of Eq.(5) into Eq.(4). We arrive at

$$\mathbf{f} = \frac{2\pi g_h}{(4\pi^2)^4} \int d\mathbf{p} \int d\mathbf{p}' \int d\mathbf{k} \int d\mathbf{k}' |u_{\mathbf{p}-\mathbf{p}'}|^2 \delta(\mathbf{p}' - \mathbf{p} + \mathbf{k} - \mathbf{k}') \delta(\varepsilon_{\mathbf{p}}^h - \varepsilon_{\mathbf{p}'}^h + \varepsilon_{\mathbf{k}'}^e - \varepsilon_{\mathbf{k}}^e) \quad (13)$$

$$\left\{ (\mathbf{p} - \mathbf{p}', \mathbf{p}) \mathbf{V}_h (-\partial_{\varepsilon_{\mathbf{p}}^h} f_{\mathbf{p}}^{(0h)}) \left[f_{\mathbf{k}}^{(0e)} (1 - f_{\mathbf{k}'}^{(0e)}) f_{\mathbf{p}'}^{(0h)} + f_{\mathbf{k}'}^{(0e)} (1 - f_{\mathbf{k}}^{(0e)}) (1 - f_{\mathbf{p}'}^{(0h)}) - \right. \right. \quad (14)$$

$$\left. \left. (\mathbf{k} - \mathbf{k}', \mathbf{k}) \mathbf{V}_e (-\partial_{\varepsilon_{\mathbf{p}}^e} f_{\mathbf{k}}^{(0e)}) \left[f_{\mathbf{p}}^{(0h)} (1 - f_{\mathbf{p}'}^{(0h)}) f_{\mathbf{k}'}^{(0e)} + f_{\mathbf{p}'}^{(0h)} (1 - f_{\mathbf{p}}^{(0h)}) (1 - f_{\mathbf{k}'}^{(0e)}) \right] \right\}$$

The integral over \mathbf{p} can be presented as $\int d\mathbf{p} = m_h \int d\varepsilon_{\mathbf{p}} \int d\varphi_{\mathbf{p}}$ and similarly for the integral over other momenta. Calculating integrals over energies in the low

temperature limit we obtain the following expression for the mean free time between collisions of holes with electrons

$$\frac{1}{\tau_{he}} \equiv \frac{N_s \eta}{m_h} = \frac{T^2 m_e^2 m_h}{(4\pi^2)^3} \frac{\zeta^2}{2P_s \hbar^7} \int_0^{2\pi} d\phi d\varphi d\varphi' (1 - \cos \phi) \delta(\zeta(\cos \phi - 1) + \cos \varphi - \cos \varphi') \times \quad (15)$$

$$\delta(\zeta \sin \phi + \sin \varphi - \sin \varphi') |u_{p_{Fh}(1-\cos \phi)}|^2,$$

where $\zeta = p_{Fh}/p_{Fe}$, p_{Fh}, p_{Fe} are the Fermi momenta of holes and electrons respectively.

Expression (15) can be transformed to

$$\frac{1}{\tau_{he}} = \frac{m_e^2}{12\pi^3 g_h \hbar^5} \frac{T^2}{\epsilon_{Fh}} \zeta \int_0^{x_0} dx \frac{x |u_{2p_{Fh}x}|^2}{\sqrt{1-x^2} \sqrt{1-\zeta^2 x^2}}. \quad (16)$$

Here $x_0 = \min(1, 1/\zeta)$.

The Fourier transform of the Coulomb e-h interaction $u_{\mathbf{q}}$ depends on the structure of the system and the screening. In the simple 2D model of electron gas the Coulomb interaction with linear screening reads as

$$u_{\mathbf{q}} = \frac{2\pi e^2}{\chi} \frac{1}{q + \kappa}, \quad (17)$$

where the screening constant is collected from the individual screening constants of electron and hole gases, $\kappa = \kappa_e + \kappa_h = 2(g_h/a_{B,h} + g_e/a_{B,e})$, $a_{B,e} = \hbar^2 \chi / m_e e^2$ and $a_{B,h} = \hbar^2 \chi / m_h e^2$ are the Bohr radii of electrons and holes, respectively; χ is the effective dielectric constant.

This expression is valid in the linear screening approximation that needs smallness of κ as compared to the transmitted momentum $\min(p_{Fe}, p_{Fh})$. Besides, here we neglect the width of the quantum well. As a result, the potential becomes independent of the HgTe dielectric constant. This 2D consideration loses applicability in the specific system under the consideration where the quantum well width $d \gtrsim 1/\kappa$. In fact, the screening radius $1/\kappa$ should be limited from below by d .

Accounting for finite width of the quantum well leads to replacement of the 2D potential by

$$u_q = \frac{2\pi e^2}{\chi} \frac{F(qd)}{q + \kappa F(qd)}, \quad q < 2(p_{Fe}, p_{Fh}). \quad (18)$$

where the function $F(qd)$ follows from the solution of electrostatic interaction problem of two singly charged particles placed inside a layer of width d between two semi-infinite dielectrics. Using planar Fourier transform, we have for the interaction of two point charges located in the points z, z' , $d/2 > z > z' > -d/2$:

$$- \frac{e^{-q(z+z')} (e^{dq}(r+1) - e^{2qz}(r-1)) (-r + e^{q(d+2z')}(r+1) + 1)}{2\chi q (e^{2dq}(r+1)^2 - (r-1)^2)}. \quad (19)$$

For $z < z'$ it is necessary to do replacements $z \leftrightarrow z'$ in Eq.(19). Here $r = \chi/\chi_{\text{HgTe}}$, χ is the dielectric constant of external layers (*CdTe*). To find the func-

tion $F(x)$, one should integrate the potential (19) with the squares of electron and hole transversal wave functions $|\psi_e(z)|^2$ and $|\psi_h(z')|^2$. For a well with hard walls

$\psi_{e,h}(z) = \sqrt{2/d} \cos(\pi z/d)$. In this case, we find

$$F(x) = \frac{r}{(x^2 + 4\pi^2)^2} \left(x(3x^2 + 20\pi^2) + 32\pi^4 \frac{(-1 + e^x)x + r(e^x(x-2) + x + 2)}{(r + e^x(r+1) - 1)x^2} \right) \quad (20)$$

Assembling the previous expressions we get the τ_{he} for the Coulomb scattering

$$\frac{1}{\tau_{he}} = \frac{m_e e^4}{6\pi \chi^2 g_h \hbar^3} \frac{m_e}{m_h} \frac{T^2}{\epsilon_{Fh}^2} \zeta \int_0^{x_0} dx \frac{x F^2(wx)}{\sqrt{1-x^2} \sqrt{1-\zeta^2 x^2} (2x + \xi F(wx))^2}, \quad (21)$$

where $w = 2p_{Fh}d$, $\xi = \kappa/p_{Fh}$. In the strict 2D case $w = 0$, the potential converts to Eq.(17) and $F(wx)$ should be replaced by 1. It should be emphasized that in the real case the parameter ξ is large, so, the mean free time ceases to depend on F . This conclusion is valid in the linear screening theory. Careful examination shows the necessity of revision of this approach. Quantity $1/\tau_{he}$ is proportional to T^2 . This results in a similar temperature dependence of the correction to the residual resistivity at low temperature.

Short-range interaction

Together with the long-range Coulomb part the interaction between electrons and holes contains also the short-range kernel interaction. Large dielectric constant of HgTe and CdHgTe leads to the dielectric screening of the Coulomb contribution. In that case the on-site e-h interaction can prevail. To estimate the kernel contribution one can replace $u_{2p_{Fh}x}$ by a constant:

$$u_{2p_{Fh}x} = \pi \hbar^2 \frac{m_e + m_h}{m_e m_h} \Lambda; \quad \Lambda = \frac{m_e m_h}{m_e + m_h} \frac{1}{\hbar^2 \pi} \int u(r) d\mathbf{r}. \quad (22)$$

Dimensionless quantity Λ describes the strength of the contact e-e-interaction. As a result we find for η :

$$\eta = \frac{(m_e + m_h)^2 \Lambda^2 T^2}{24\pi^2 \hbar^3 N_s P_s} \ln \left| \frac{1+\zeta}{1-\zeta} \right| \quad (23)$$

In accordance with (15), the model of isotropic energy spectrum leads to a logarithmic divergency of the temperature corrections to the conductivity at equal Fermi

momenta of electrons and holes. The divergency originates from the probability of two Fermi particle backscattering with conservation of their individual energies. For the isotropic Fermi surfaces such processes occur for all electrons on the Fermi surface.

Anisotropic spectrum

In fact, the holes in the system under consideration have anisotropy. That evidently limits kinematically the possibility of backscattering and the divergency. This makes it necessary to take into account the hole spectrum anisotropy neglected before. It can be done in the relaxation time approximation for elliptic hole spectrum for the case of zero magnetic field. The anisotropy of the spectrum results in the anisotropy of temperature corrections. In accordance with the experimental situation, we shall consider the electric field applied along the symmetry axes, say i . In this case Eq.(7) is modified as

$$\frac{e}{m_i} E_i - \frac{V_i^h}{\tau_h} - \eta \frac{P_s}{m_i} (V_i^h - V_i^e) = 0. \quad (24)$$

Here, subscript i marks the specific direction of the field and the same component of the hole mass.

Friction coefficient η_i for the same direction of electric field reads

$$\eta_i = \frac{m_h}{N_s \tau_{he,i}} = \frac{T^2 (m_e + m_h)^2 \Lambda^2}{6\pi^3 \hbar^3 N_s P_s} f(\alpha_i, \zeta), \quad (25)$$

where $m_h = \sqrt{m_1 m_2}$ is the mass of the hole density of states, $\alpha_i = \sqrt{m_i/m_h}$,

$$f(\alpha, \zeta) = \frac{(\alpha\zeta)^2}{32} \int_0^{2\pi} d\varphi d\varphi' d\phi d\phi' (\cos \varphi - \cos \varphi') \delta(\alpha\zeta(\cos \varphi' - \cos \varphi) + \cos \phi - \cos \phi') \times \delta((\zeta/\alpha)(\sin \varphi' - \sin \varphi) + \sin \phi - \sin \phi'). \quad (26)$$

Integrals over three angles can be evaluated and we arrive at

$$f(\alpha, \zeta) = \alpha^4 \int_0^1 \frac{x^2 dx}{\sqrt{1-x^2}(1+x^2(\alpha^4-1))} \ln \left| \frac{\alpha + \zeta \sqrt{1+x^2(\alpha^4-1)}}{\alpha - \zeta \sqrt{1+x^2(\alpha^4-1)}} \right|. \quad (27)$$

Fig.2 shows the dependence of $f(\alpha, \zeta)$ on ζ for different α . All curves contain the limited singularities corresponding to the equality of the hole Fermi ellipses axes to the diameter of the electron Fermi circle. The exception is the case of $\alpha = 1$, when $f(1, \zeta) \propto -\ln|\zeta - 1|$ at $\zeta \rightarrow 1$. In this case, the divergency can be limited by the finite temperature or collision widening.

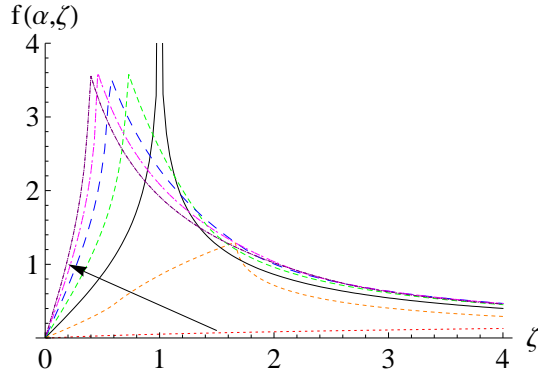


FIG. 2: Dependence of temperature correction in the anisotropic case on the electron-to-holes concentration ratio and the hole masses ratio via parameters ζ and α . Parameter α runs values 0.2, 0.6, 1, 1.4, 1.8, 2.2, 2.6. The irection of α growth is shown by arrow.

II. EXPERIMENT

Samples

The $Hg_{0.3}Cd_{0.7}Te/HgTe/Hg_{0.3}Cd_{0.7}Te$ quantum wells with the (013) surface and the thickness of 20.5 nm were prepared by molecular beam epitaxy. The details of the structure growth process are described in [8, 9]. The QW cross-section and the energy diagram of the structures investigated is shown in Fig.3a and 1b,

respectively. To perform magnetotransport measurements, the samples based on these quantum wells were prepared by standard photolithography in the form of 50 μm wide Hall bars with the voltage probes spaced 100 μm apart. The ohmic contacts to the two-dimensional gas were formed by the in-burning of indium. To change and control the electron and hole densities in the QW, the electrostatic top gate has been supplied. For this purpose, a dielectric layer containing 100 nm SiO_2 and 200 nm Si_3N_4 was first grown on the structure using the plasma-chemical method. Then, the TiAu gate was deposited. The schematic drawing of the devices prepared in this way is shown in Fig.3c. The magnetotransport measurements in the described structures were performed in the temperature range of 0.2–4.1 K in magnetic fields up to 5 T by the standard four-point circuit at the 12–13 Hz ac signal with the current of 1–10 nA through the sample, which is sufficiently low to avoid the overheating effects.

Experimental results

To gather information about the structures properties and to determine the main transport parameters of the system corresponding to different gate voltages, the magnetic field dependences of the diagonal $\rho_{xx}(B)$ and Hall $\rho_{xy}(B)$ components of the resistance tensor were measured. These functions show a strong dependence on the magnitude and sign of the gate voltage applied to the sample. Fig.4a,b,c present the curves measured at gate voltages -3, -1.84 and -0.5 V respectively. One can see that an alternating-sign Hall effect and strong positive magnetoresistance are observed at $V_g = 3$ and -1.84 V (see Fig.4a,b). Meanwhile, at $V_g = -0.5$ V (see Fig.4c), there is a weak negative magnetoresistance at low fields and positive magnetoresistance at higher fields, and the magnetic field dependence of the Hall resistance is linear with its slope opposite to that of $\rho_{xy}(B)$ at $V_g = 3$ and

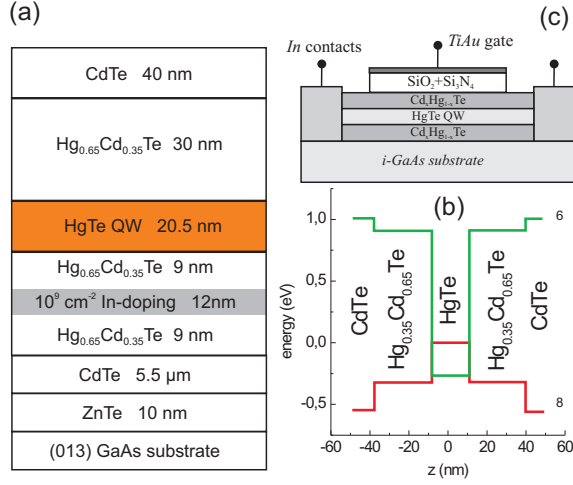


FIG. 3: The quantum well layer structure - (a), the quantum well energy diagram -(b), and the cross section of the samples studied.

-1.84 V and $|B| > 0.1$ T and $|B| > 0.4$ T, respectively.

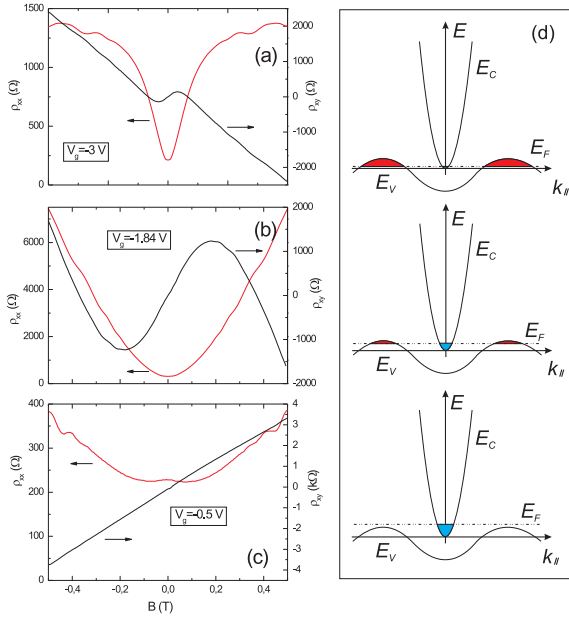


FIG. 4: Magnetic field dependences $\rho_{xx}(B)$ and $\rho_{xy}(B)$ for the 2D electron-hole system in the HgTe quantum well at $T = 0.19$ K for three gate voltages: (a)- $V_g = -3$ V; (b)- $V_g = -1.84$ V and (c)- $V_g = -0.5$ V; (d)- the energy band diagrams with approximate positions of the Fermi energy corresponding to the curves on the left side.

The described behavior suggests that, by varying the gate voltage we change the carrier type content in the quantum well. This conclusion is further supported by the $\rho_{xx}(V_g)$ and $\rho_{xy}(V_g)$ traces measured at a constant

magnetic field $B = 2$ T corresponding to the quantum Hall effect regime, Fig.5. The quantum Hall plateaux in $\rho_{xy}(V_g)$ and minima in $\rho_{xx}(V_g)$ are well developed for filling factors $\nu = 1 - 10$ on the electron side and for $\nu = 1 - 4$ on the hole side indicating a very high quality of the samples investigated. At $V_g \approx -1.8$ V a dramatic change of the sign of ρ_{xy} takes place signifying a change of the predominant carrier type in the well. This transformation in $\rho_{xy}(V_g)$ is accompanied by a sharp peak in $\rho_{xx}(V_g)$. The behavior of our system in the quantum Hall effect regime has been studied earlier [10].

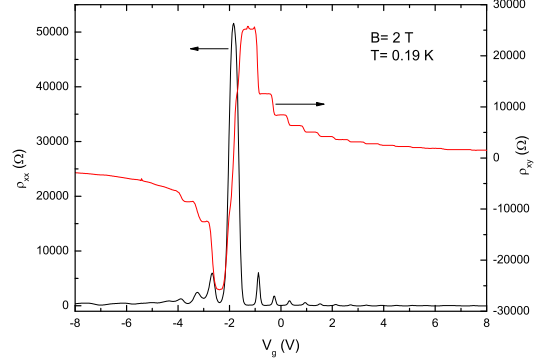


FIG. 5: Gate voltage dependences $\rho_{xx}(B)$ and $\rho_{xy}(B)$ for the 2D electron-hole system in the HgTe quantum well at $T = 0.19$ K and magnetic field $B = 2$ T.

By fitting the dependences similar to those presented in Fig.4a,b,c using the formulas of the standard classical transport model in the presence of two groups of carriers of opposite signs [11], we can determine the types of charge carriers involved in the transport, as well as their mobilities and densities. Fig.6 presents these parameters as functions of the gate voltage. We first consider the gate voltage dependences of the electron and hole densities shown in Fig.6a. For $V_g \geq -1$ V, the experimental curves (see, e.g., Fig.4c) are adequately described by the transport model involving only electrons as charge carriers. Although holes can be present in this case with a density much lower than the electron density, their contribution to the transport is immaterial due to their lower mobility. As would be expected, the gate voltage dependence of the electron density is linear with a slope of $8.12 \times 10^{14} m^{-2} V^{-1}$ corresponding to the capacitance of the dielectric. An absolutely different pattern is observed for $V_g \leq -1.5$ V. To describe the dependences similar to those presented in Fig.4a,b two types of carriers, electrons and holes, should be taken into account. Fig.6a shows the electron and hole densities as functions of the gate voltage for $V_g \leq -1.5$ V obtained from the processing of the experimental data. Clearly, as the negative gate bias increases, the hole density increases and the electron density decreases linearly with slopes 7.9×10^{14}

and $0.7 \times 10^{14} \text{ m}^{-2} \text{ V}^{-1}$, respectively. We note that the sum of the magnitudes of these slopes is about the magnitude of the slope of $N_s(V_g)$ for $V_g \geq -1 \text{ V}$, as would be expected, because electrons are the only observable type of carriers for $V_g \geq -1 \text{ V}$. Moreover, the slope ratio $P_s(V_g)/N_s(V_g) \approx 11.3$ for $V_g \leq -1.5 \text{ V}$ should correspond to the ratio of the densities of states of holes and electrons. Then, if holes fill two valleys (as expected for a (013) 20 nm HgTe QW) and electrons fill only one valley, then the hole mass is $m_h \approx 0.15m_0$ if we take the electron mass $m_e \approx 0.025m_0$. These values are close to those determined from the cyclotron resonance measurements [12].

Processing diagonal $\rho_{xx}(B)$ and Hall $\rho_{xy}(B)$ dependences in the vicinity of the gate voltages where the electron and hole densities are close is rather difficult. However, extrapolating linear dependences $N_s(V_g)$ and $P_s(V_g)$, we find their crossing point, where the electron and hole densities are equal, $V_g \approx -1.3 \text{ V}$ - the so called charge neutrality point (CNP).

Using the electron and hole density versus gate voltage dependences obtained above we can plot the opposite to Fig.4a,b,c qualitative energy band diagrams with the corresponding Fermi level positions and the conduction and valence band occupation, Fig.4d. As mentioned above for the (013) HgTe QWs we have a single conduction band minimum in the center of the Brillouin zone and two valence band maxima situated along the [0-13] direction. According to the CNP electron and hole densities and their mass values determined above the conduction and the valence bands overlap in our samples is about 10 meV.

Now, we consider the behavior of the electron and hole mobilities as V_g varies (see Fig.6b). The lines are drawn through the experimental points for visualization. In the range of $-1.5 \text{ V} \leq V_g \leq +3 \text{ V}$, a decrease in the electron density is accompanied by a marked decrease in their mobility roughly as $\sim N_s^{3/2}$. Similar dependency of mobility on density is frequently observed in other two-dimensional structures as well, where the carrier density is controlled by the electrostatic gate. It results from the transport time for impurity scattering depending on the carrier density as $\tau_{tr} \approx N_s^\alpha$, where $\alpha = 1 - 2$. In the gate voltage range of $-2 \leq V_g \leq -1.5 \text{ V}$ corresponding to the approximate equality of the electron and hole densities, a sharp jump in the electron mobility is observed (see the dotted line in Fig.6b). A further increase in the magnitude of the negative gate bias slightly reduces the electron mobility and weakly increases the hole mobility. Of the most interest is the jump in electron mobility at $-2 \leq V_g \leq -1.5 \text{ V}$. This jump coincides with the gate voltage range where the hole density first equals and then begins to exceed the electron density: $P_s \geq N_s$. We suggest that this jump may be accounted for by the holes screening and, therefore, reducing impurity scattering of electrons.

As shown in Section I, in a bipolar system with two types of charge carriers of the opposite sign, momentum

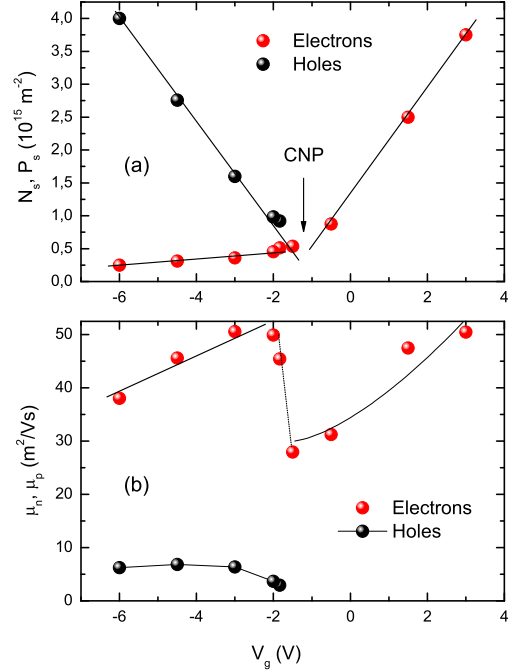


FIG. 6: (a)- the electron N_s and hole P_s densities versus gate voltage; (b)- the electron μ_n and hole μ_p mobilities versus gate voltage; $T = 0.19 \text{ K}$.

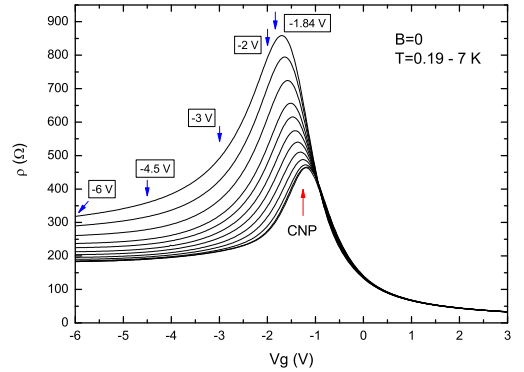


FIG. 7: Gate voltage dependences $\rho(V_g)$ at $B = 0$ and various temperatures $T =$ (from bottom to top) $T = 0.2; 0.5; 1; 1.5; 2; 2.5; 3; 3.6; 4.1; 5; 6; 7 \text{ K}$.

relaxation can be caused, in addition to other factors, by their mutual scattering (friction) [5]. Since only the particles of both kinds that fall into the kT interval in the vicinity of the Fermi level are involved in this momentum relaxation mechanism, the corresponding relaxation time is expected to change with temperature as $\sim T^{-2}$.

Fig.7 presents the gate voltage dependences of our sample resistance in the zero magnetic field for a number of temperatures in the interval $T = 0.19 - 7$ K. Each $\rho(V_g)$ curve has a pronounced maximum. At the lowest temperature $T = 0.19$ K, the position of this maximum almost coincides with the gate voltage at which the hole and electron densities are equal (CNP). Another interesting feature of the curves in Fig.7 is their asymmetric temperature dependence with respect to the gate voltage. One can see that for $V_g \geq -1$ V, i.e. when the electrons are the only detectable carriers in the system, there is only a weak dependence of resistance on temperature. Meanwhile, at $V_g \leq -1$ V, i.e. when the holes begin to populate the valence band, a considerable increase (by a factor of 1.5 - 3) in resistance is observed as the temperature increases from 0.2 K to 7 K. It is maximal in the range of $-3\text{V} \leq V_g \leq -1$ V and decreasing for higher negative gate biases. Also, with the temperature increasing the maximum of the $\rho(V_g)$ curve shifts by about 0.5 V to negative gate voltages. In the following section we analyze the observed behavior using the theory of electron-hole scattering developed in Section I.

III. THEORY VERSUS EXPERIMENT

Due to the electron-hole scattering, there would be a stronger temperature dependence of the resistivity in the gate voltage range where both holes and electrons are present $V_g \leq -1$ V compared to $V_g \geq -1$ V, where the electrons are the only charge carriers (see Fig.6a). To analyze the system behavior at $V_g \leq -1$ V, we use Eq.(12) from Section I, obtained for the temperature dependence of resistance in a system with two types of charge carriers when the momentum relaxation is due to their mutual scattering, which we rewrite in the following form:

$$\rho(T) = \rho_0 \frac{1 + (\eta/e)(N_s\mu_p + P_s\mu_n)}{1 + (\eta/e)(N_s - P_s)^2\mu_n\mu_p/(N_s\mu_n + P_s\mu_p)} \quad (28)$$

Here, ρ_0 , N_s , P_s , μ_n , and μ_p are the system resistance, the electron and hole densities and mobilities at $T = 0$, respectively and η is the electron-hole friction coefficient defined in Sec.I. Irrespective of the details of the scattering mechanism, at specified values of the electron and hole densities the probability of electron-hole scattering decreases as the square of temperature, $\eta = \Theta \cdot T^2$, where Θ is a certain T -independent function of N_s and P_s to be determined.

In Fig.8a we plot with closed circles the $\rho(T)$ dependences obtained from the experimental curves in Fig.7 at $V_g = -1.84; -2; -3; -4.5; -6$ V (in Fig.7 these gate voltages are marked with arrows). For all these gate voltages, the resistivity temperature dependence saturates at $T \leq 0.5$ K. This allows us to use the values of the electron and hole mobilities and densities at these temperatures as zero-T quantities in Eq.(28) when fitting it to the experimental data in Fig.8a. For each of the specified gate

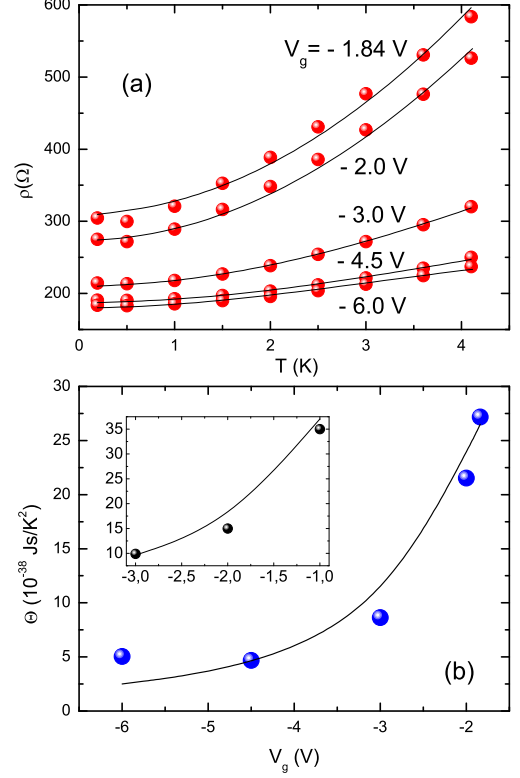


FIG. 8: (a)-Temperature dependences $\rho(T)$ obtained from Fig.7 for $V_g = 1.84, 2, 3, -4.5, -6$ V (marked with arrows in Fig.7). The lines are the fitting by Eq.(28) (see the text); (b)-Parameter Θ obtained from fitting the experimental data in Fig.7 with Eq.(28). The solid line represents the theory given by Eqs.(25-27) with $\alpha = 1.2$ and the contact interaction constant $\Lambda = 1.36$. Insert: similar experimental data from another sample published previously [4], the line corresponds to Eqs.(25-27) with $\alpha = 1.2$ and the contact interaction constant $\Lambda = 1.64$.

voltages these zero-T parameters were independently obtained from the magnetotransport data as described in the above discussion of the curves in Fig.4a,b,c. Therefore, the fitting procedure for each value of the gate voltage in Fig.8a depends on a single parameter Θ in the expression for η . The fitting of Eq.(28) to the data is shown in Fig.8a by lines. The temperature range for fitting was chosen as 0.19-4.1 K. It was found that Eq.(28) does not fit well the experimental points for the temperatures higher than 4.1 K possibly because of other temperature dependent scattering mechanisms emerging at these temperatures. The points in Fig.8b show fitting parameter Θ as a function of the gate voltage. In the insert we show, for statistics, a similar data for another sample that was published previously [4].

Let us now apply the theoretical results obtained in Sec.I for the analysis of the gate voltage dependence of

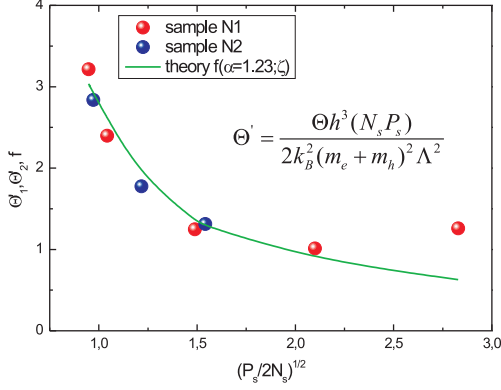


FIG. 9: Dimensionless quantity $\frac{\Theta h^3 N_s P_s}{2k_B^2 (m_e + m_h)^2 \Lambda^2}$ plotted as a function of $\zeta = \sqrt{P_s/2N_s}$ for the two samples data in Fig.8b. The solid line represents the theory, Eq.(27).

$\Theta = \eta/T^2$. Before we begin, it is vital to note that parameter Θ gives a first hand information about the interparticle interaction which makes our situation rather unique. Indeed, in the general case of a 2D electron system with $\sigma \gg e^2/h$ this information can only be obtained from the study of quantum corrections which, apart from being only few percent of the total conductivity depend on the interaction in an indirect and complicated form [13–15].

First of all we notice that the weak e-h interaction approximation of our theory, given by Eq.(21), does not seem to be applicable in our case. Indeed, a direct calculation of Θ using Eq.(21) for our system parameters and the corresponding values of N_s , P_s yields Θ about two orders of magnitude less than that observed experimentally (Fig.8b). The reason for this is probably related to the following fact. In the carrier density range investigated, the ratio of the screening constant to the Fermi wave vector $\kappa/\min(p_{Fh}, p_{Fe}) \approx 20 \gg 1$ in which case treating the e-h interaction as weak becomes unjustified. Besides, $1/\kappa = 1.3 \text{ nm} \ll d$, where $d = 20 \text{ nm}$ is the QW width, and the 2D consideration loses applicability.

We have taken into theoretical consideration a variety of factors affecting the e-h interaction, except for its large strength. Besides the general difficulties associated with the consideration of strong interaction in a simple 2D case, there are complications due to the specificity of HgTe quantum wells.

In fact, the individual electron energy levels and wave functions in a narrow-gap semiconductor are obtained from the size quantization of a many-component wave function, that results in a complicated space dependence of electron density. Owing to the large strength of e-h interaction, its essential part is accumulated on distances comparable to the well width. This factor strongly mod-

ifies the Coulomb interaction. The long-range components of the Coulomb interaction are suppressed, while a short-range 2D scattering amplitude is formed on the scale of the well width.

Under these circumstances we can consider the e-e scattering in the simplest way, and turn to the short-range potential model represented by Eq.(23) for the isotropic case and by its extension (Eqs.(25-27)) for the anisotropic spectrum. Then we have only a single fitting parameter Λ , the value of which can not be found in the 2D model developed here.

The solid lines in Fig.8b and the Insert are the fitting of Eqs.(25-27) to the experimental dependences of $\Theta(V_g)$ with $\Lambda = 1.36$ (1.64 for the data in the Insert) and the hole mass anisotropy coefficient $\alpha = 1.2$ in both cases. A more universal way to present the data is to plot quantity $\frac{\Theta h^3 N_s P_s}{2k_B^2 (m_e + m_h)^2 \Lambda^2}$ as a function of $\zeta = \sqrt{P_s/2N_s}$, in which case the experimental points for both of the samples should fall on the same curve $f(\alpha, \zeta)$. As one can see in Fig.9, this is indeed the case.

The values of Λ obtained from the fitting in Fig.8b appear to be too large if we assume that it represents Coulomb interaction with the dielectric constant of HgTe equal to 12-15. At the same time, these values are in good agreement with the short-range model considerations.

Let us discuss the origin of short-range interaction in more detail. In quantum wells of conventional semiconductors the subbands are formed from the simple envelope-function states. On the contrary, in a HgTe quantum layer the size quantization and the formation of a gap occur simultaneously. The e-h interaction modifies the bands, and the value of the effective e-h interaction is inevitably related to the structure of the states. This determines the characteristic energy and spatial scales of the e-h interaction, namely, the gap as the characteristic energy scale and the width of the quantum layer as the length scale. That results in a value of Λ comparable with the extracted from the experimental data.

It should be emphasized, that a large e-e interaction constant means the inapplicability of the Born approximation for the electron-hole pair scattering and of the Fermi gas concept. However, constant Λ can be treated as a low-energy limit of a dimensionless scattering amplitude that preserves the above-mentioned estimates. In fact our results constitute an evidence that even in the case of $\sigma \gg e^2/h$ a 2D e-h system in HgTe QW should be considered as a strongly correlated 2D e-h liquid rather than a 2D e-h gas.

IV. CONCLUSIONS

We have developed the theory of temperature-dependent corrections to the conductivity and magnetotransport coefficients in a 2D semimetal. These corrections are caused by friction between electrons and holes. The corrections obey the quadratic temperature dependence at the low temperature limit. The friction

coefficients are found for the linear-screened Coulomb electron-hole interaction and the real spatial structure of the system. Besides, calculations have been made for the core electron-hole scattering in the assumption that the Coulomb potential is completely screened. The experiments were performed in 20 nm (013) HgTe QW. We found that the conductivity variation with temperature due to electron-hole scattering is very large (2-3 times higher than the conductivity in the zero temper-

ature limit). This gives us the opportunity to obtain a direct information about interparticle interaction in a 2D electron-hole system with a high ($\sigma \gg e^2/h$) conductivity value. It has proved to be impossible to explain the observed strong temperature dependent variation of conductivity as a consequence of electron-hole scattering due to Coulomb interaction. Instead, the short-range e-h scattering model was found to be satisfactory for the explanation of the observed large friction strength.

-
- [1] Z. D. Kvon, E. B. Olshanetsky, D. A. Kozlov, et al., Pisma Zh. Eksp. Teor. Fiz. **87**, 588 (2008) [JETP Lett. **87**, 502 (2008)].
 - [2] Z. D. Kvon, E. B. Olshanetsky, E. G. Novik, D. A. Kozlov, et al., Phys. Rev. B **83**, 193304 (2011).
 - [3] E. B. Olshanetsky, Z. D. Kvon, N. N. Mikhailov, et al., Solid State Comm. **152**, 265 (2012).
 - [4] E. B. Olshanetsky, Z. D. Kvon, M. V. Entin et al., Pisma Zh. Eksp. Teor. Fiz. **89**, 338 (2009); [JETP Lett. **89**, 290 (2009)].
 - [5] V. F. Gantmakher, I. B. Levinson, Carrier Scattering in Metals and Semiconductors (Nauka, Moscow, 1984; North Holland, New York, 1987).
 - [6] V. F. Gantmakher, I. B. Levinson, Zh. Eksp. Teor. Fiz. **74**, 261 (1978) [JETP **47**, 133 (1978)].
 - [7] M. V. Entin, L. I. Magarill, Eur. Phys. J. B **81**, 225 (2011).
 - [8] N. N. Mikhailov, R. N. Smirnov, S. A. Dvoretzky et al., Int. J. Nanotechnology **3**, 120 (2006).
 - [9] E. B. Olshanetsky, S. Sassine, Z. D. Kvon et al., Pisma Zh. Eksp. Teor. Fiz. **84**, 661 (2006) [JETP Lett. **84**, 565 (2007)].
 - [10] G. M. Gusev, E. B. Olshanetsky, Z. D. Kvon, A. D. Levin, N. N. Mikhailov, and S. A. Dvoretzky, Phys. Rev. Lett. **108**, 226804 (2012).
 - [11] V. L. Bonch-Bruевич and S. G. Kalashnikov, Semiconductor Physics (Nauka, Moscow, 1990) [in Russian].
 - [12] D. A. Kozlov, Z. D. Kvon, N. N. Mikhailov, S. A. Dvoretzky, and J. C. Portal, Pisma Zh. Eksp. Teor. Fiz. **93**, 186 (2011), [JETP Lett. **93**, 170 (2011)].
 - [13] B. L. Altshuler, A. G. Aronov, Electron-electron interactions in disordered systems, Edited by A. L. Efros, M. Pollak, Elsevier Science Publishers B. V., 1985.
 - [14] A. M. Finkelstein, JETP Lett. **37**, 517 (1983).
 - [15] G. Zala, B. N. Narozhny, and I. L. Aleiner, Phys. Rev. **B64**, 214204, (2001).